

INVESTIGATIONS OF OPERATION PROBLEMS AT A 200 MWE PF BOILER

Sandile Peta^{1*}, Chris du Toit², Reshendren Naidoo³, Walter Schmitz³,
Louis Jestin⁴

¹ ESKOM SOC, Group Technology Engineering, Boiler Auxiliaries, 1 Simba Rd, Sunninghill, Johannesburg, South Africa

² ESKOM SOC, Generation Engineering, Camden Power Plant, Ermelo, South Africa

³ University of Witwatersrand, School of Mechanical, Industrial and Aeronautical Engineering, Johannesburg, South Africa

⁴ University of Cape Town, Faculty of Engineering and the Built Environment, Cape Town, South Africa

To minimize oxides of nitrogen (NO_x) emission, maximize boiler combustion efficiency, achieve safe and reliable burner combustion, it is crucial to master global boiler and at-the-burner control of fuel and air flows. Non-uniform pulverized fuel (PF) and air flows to burners reduce flame stability and pose risk to boiler safety by risk of reverse flue gas and fuel flow into burners. This paper presents integrated techniques implemented at pilot ESKOM power plants for the determination of global boiler air/flue gas distribution, wind-box air distribution and measures for making uniform the flow being delivered to burners within a wind-box system. This is achieved by Process Flow Modelling, at-the-burner static pressure measurements and CFD characterization. Global boiler mass and energy balances combined with validated site measurements are used in an integrated approach to calculate the total (stoichiometric + excess) air mass flow rate required to burn the coal quality being fired, determine the actual quantity of air that flows through the burners and the furnace ingress air. CFD analysis and use of at-the-burner static, total pressure and temperature measurements are utilized in a 2-pronged approach to determine root-causes for burner fires and to evaluate secondary air distribution between burners.

Keywords: process flow modelling, mass and energy balance, furnace CFD modelling, PF swirl burner

1. INTRODUCTION

ESKOM's Camden boilers (Fig. 1) were manufactured by International Combustion Africa Limited (ICAL) and are of the two-pass drum type without reheat. The power plant design capacity is 8×200 MWe with a boiler acceptance test efficiency measured at 88.44%. Each boiler is front-wall fired by 20 Type 'R' swirl burners which are fed by 5 vertical spindle mills which have static classifiers and a multi-turret outlet. Full load electrical output is achieved by 4 mills and 16 burners. The boilers were commissioned in the late 60's and mothballed in the late 80's due to surplus power generation capacity. Due to a sharp increase in power demand in the mid to late 90's and constraints on South Africa's existing power generation capacity (Winkler, 2006), the units were returned to service (RTS) with the first unit (Unit 6) being re-commissioned in March 2005 and the final units (Unit 1 and 2) in early 2008.

* Corresponding author, email: sandile.peta@gmail.com

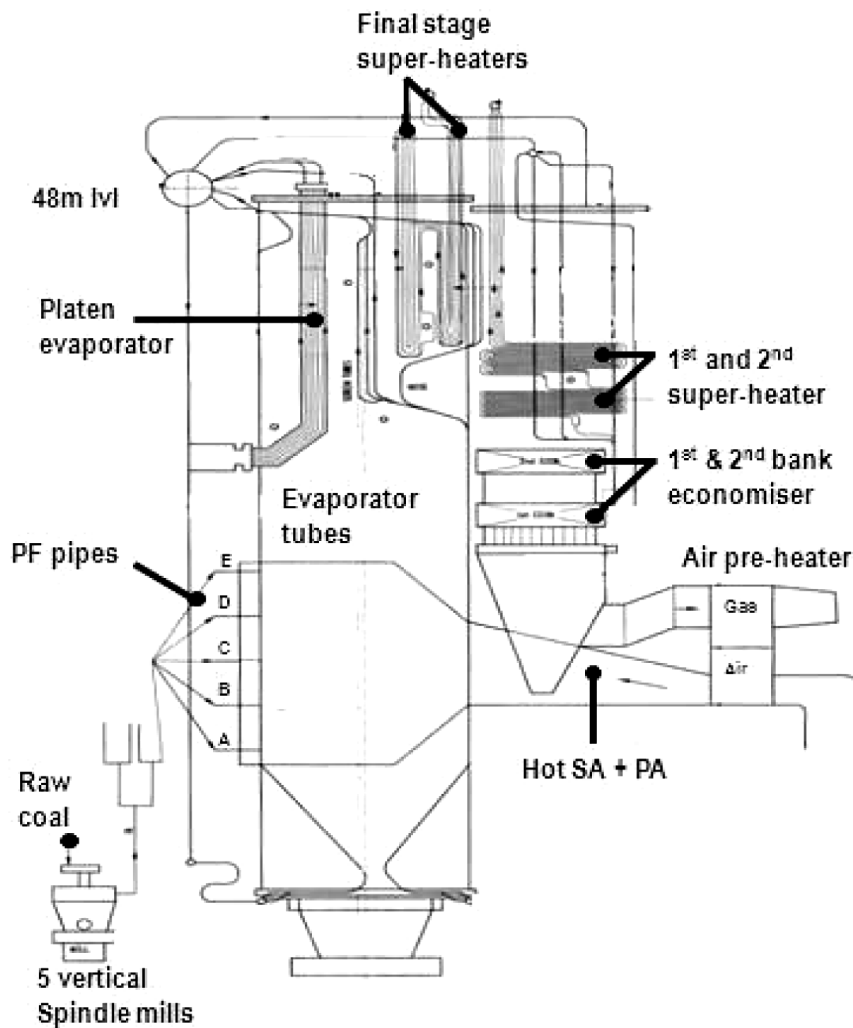


Fig. 1. Sectional side view of Camden boiler elevation

Prior to the power plant being mothballed, the boilers suffered mainly from furnace slagging, super-heater metal temperature excursions, and fabric filter plant temperature excursions. These drawbacks have continued to plague the plant during the post-mothballing era, leading to plant load reduction, unavailability and reduced remnant life of high temperature pressure parts and Fabric Filter Plant (FFP). This paper hereafter describes the measures implemented on the global boiler, combustion system and burners, during and following the RTS period in an attempt to understand the drawbacks and improve the performance. Furthermore a discussion of the results obtained thus far and further work to be undertaken is given.

2. INVESTIGATION STRATEGY

The investigation approach was structured to acquire, develop and utilise engineering capabilities and tools required at 3 levels and with the following objectives:

- *Global boiler*: To establish clear coal-air-flue gas mass and energy balances and process flow models coupling the flue gas and water-steam circuits,
- *Combustion system*: To monitor, control, set and optimally operate the full set of mills and burners using insight from Computational Fluid Dynamics (CFD) tools, on-line coal and air measurements and control instrumentation,
- *Burner*: To review the designs and settings to achieve stable and well mastered combustion using mainly local measurements and insight from CFD tools.

3. GLOBAL BOILER

3.1. Mass and energy balances

In order to establish a coherent set of coal air and flue gas data, mass and energy balances (MEB) of the boiler are developed. This MEB is based on the coal chemical energy input required to raise the boiler steam to the required enthalpy while accounting for system losses (flue gas, unburnt carbon and ambient). The results of this MEB analysis were compared against validated site measurements. As shown in Fig. 2, comparison of the Boiler MEB calculated coal flow (29.2 kg/s) vs. the Distributed Control System (DCS) measured coal flow (26.5 kg/s) gives a difference of 9.2%. Given that coal flow at the plant is measured using a volumetric coal feeder, this difference has been considered as practically acceptable. A more significant discrepancy however exists, when comparing the Boiler MEB calculated combustion air requirement, to the DCS summation of the air inputs to the boiler. The Boiler MEB calculated combustion air flow is 235.0 kg/s compared to 208.0 kg/s given by the DCS at burner outlet. The 27 kg/s air mass balance discrepancy has been attributed to un-measured tramp/ ingress air through the tangent tubes in the furnace and furnace back-pass. The air ingress mass flow has been validated by a furnace pressurization leak test performed during a short duration boiler outage.

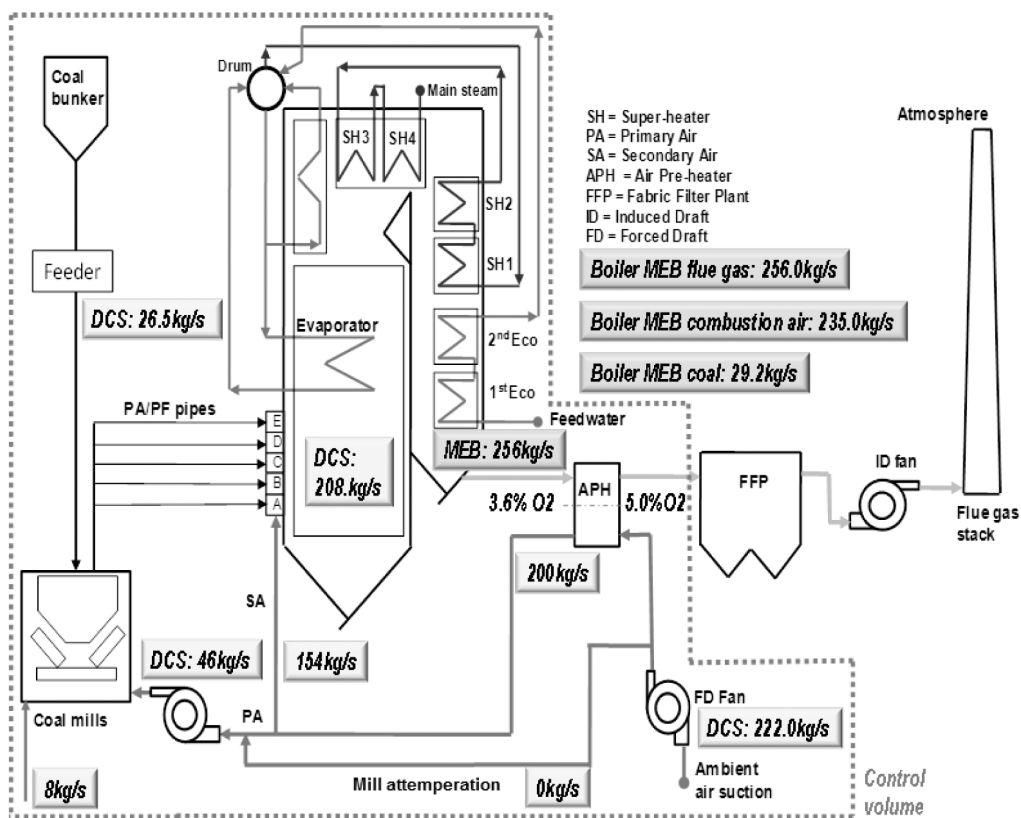


Fig. 2. Schematic of Boiler MEB analysis

3.2. Process flow modelling

In addition to the in-house Boiler MEB which has been performed, a proprietary Process Flow Model (PFM) has been used to calculate the elemental heat transfer, medium flows (mass flow rates and analyses) and specific enthalpies. This PFM couples the heat transfer between the air/flue gas streams and the water/steam circuit. The boundaries of the water/steam circuit lie between the feed-water inlet to the boiler and superheat steam outlet to the turbine. The boundaries of the air/flue gas circuit lie between forced draft fan

air inlet and the induced draft fan gas inlet. The PFM developed for Camden PS has been calibrated using site DCS process measurements as well as velocity weighted temperature measurements from a radiation shielded, multi-thermocouple matrix installed in the flue gas path at the economizer level. The multi-thermocouple matrix comprises 24 thermocouples at economizer inlet and 24 thermocouples at economizer outlet. Fig. 3a shows a photo of the economizer inlet with the thermocouple matrix installed. Fig. 3b shows the measured gas temperature profile at the economizer inlet. It is shown that the gas temperature profile is uneven in the back-pass with the maximum temperature occurring towards the front (furnace side) of the back-pass and minimum temperature occurring towards the rear of the back-pass. The velocity weighted average temperatures measured at inlet and outlet of the economizer are 595.1°C and 366.0°C respectively. Fig. 4 shows the PFM calculated air/flue gas and water steam temperature profiles across the various heat exchangers in the boiler path. The relative size of the heating surfaces is shown on the horizontal axis. Based on the introduction of the ingress air quantity (determined from comparison of the Boiler MEB and plant measurements) into the flue gas path in the PFM, good correlation between the measured and calculated average flue gas temperature at the economizer level is obtained. The PFM calculated flue gas temperatures at economizer inlet and outlet were 627.7°C and 372.9°C respectively. This gives a difference between calculation and measurement of 32.6°C and 6.9°C at economizer inlet and outlet respectively. From the PFM model, the furnace exit gas temperature is found to be 1254.8°C. This temperature is 88.8°C greater than the 1166°C specified in plant C-Schedules which contain the original design data.

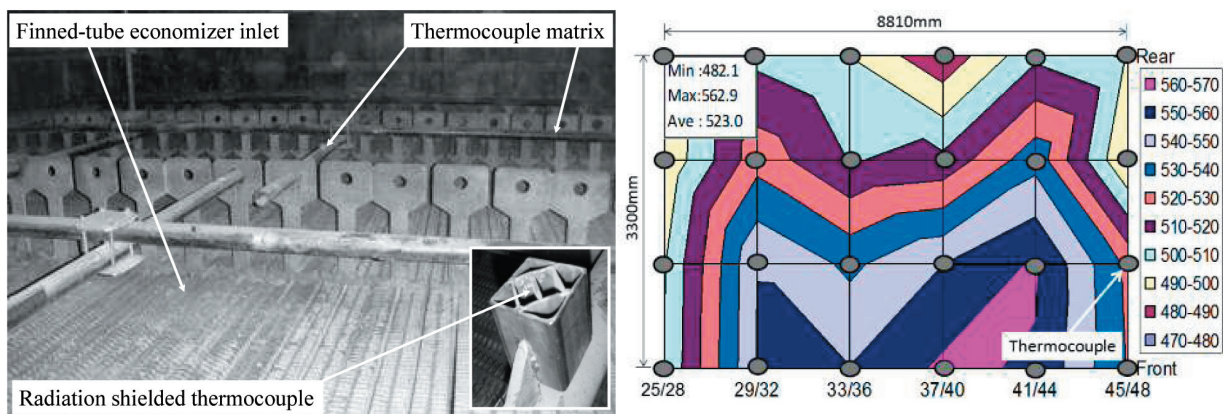


Fig. 3. a) Eco thermocouple matrix, b) Eco inlet flue gas temperature profile

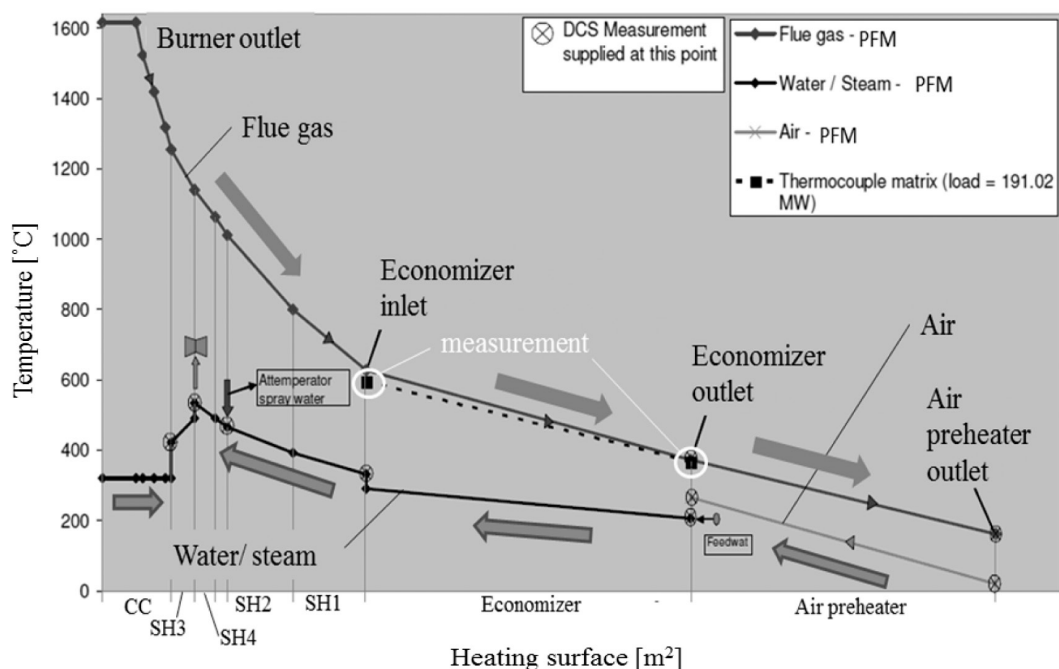


Fig. 4. Air/flue gas and water/steam profiles

3.3. Benchmarking of Camden with Rybnik power plant

The discrepancy in furnace exit gas temperature between the design value and the validated PFM calculated value prompted a design review of the combustion chamber. For the design review, RAFAKO's Rybnik power plant in Poland has been used for comparison.

Table 1 compares Rybnik and Camden power plant design and operating parameters. According to the design dimensions and operating parameters given in this table, it can be determined that the Camden boilers have an average design coal furnace residence time, between the upper row of burners till the combustion chamber exit, of around 1.27 seconds (assuming zero slip velocity between the coal particles and flue gas). The nowadays average furnace residence time is around 1.34 seconds, when taking into

Table 1. Comparison of Camden and Rybnik power plant design and operating parameters

Parameter		Power station design and operating figures		
		Camden SA	Camden SA	Rybnik Poland
	Units	Boiler		
Date	[-]	1972 (Design)	2010*	2007
Manufacturer	[-]	ICAL	ICAL	RAFAKO
Type	[-]	2-Pass	2-pass	2-Pass
Circulation	[-]	Natural	Natural	Natural
Burners (no. and configuration)	[-]	20 front fired	20 front fired	24 front fired
Load (Gross)	[MWe]	200	~195	218
		Coal analysis (air dried)		
Gross calorific value (HHV)	[MJ/kg]	24.7	20.5	-
		Raw/ as received analysis		
Net calorific value	[MJ/kg]	-	18.55	20.54
Ash content	[%]	-	29.33	28.78
Volatile content	[%]	-	19.34	22.84
Fixed carbon content	[%]	-	42.74	38.9
Total moisture	[%]	-	8.59	9.48
Total	[%]	-	100	100
		Performance		
Superheat steam pressure	[MPa]	11.03	10.65	13.65
Superheat steam temperature	[°C]	543	534.22	540
Reheat temperature	[°C]	-	-	540
Superheat steam flow	[kg/s]	206.6	201.09	181
Atmospheric pressure	[kPa]	83.5	83.5	101.3
Coal flow	[kg/s]	24.63	27.39	27.14
Combustion air (calculated)	[kg/s]	226.92	235.0	223.7
Excess air	[%]	25.6	17.95	18.75
Burner rating (calculated)	[MWth]	37.3	37.3	38
Furnace gas out temp. (mean)	[°C]	1166	1263.95**	1244***
Furnace residence time (calc.)	[s]	1.27	1.34	2.18
Economiser gas out temp.	[°C]	323	345	348
Unit efficiency	[%]	29	-	37

* Typical operating performance figures for Camden Unit 2 boiler

** Average plant pyrometer readings

*** RECOM 2-phase reactive flow CFD calculation

account a flue gas flow through the combustion chamber cross-section of 226.9 kg/s at full load (200 MWe). The difference in coal particle furnace residence time is marginal, considering that the burnout time of the coal fired in these boilers is typically around 1.2-1.4 seconds as measured in ESKOM's Drop-Tube-Furnace (DTF) at the ESKOM Research Testing and Development (RT&D) department. It is further shown in Table 1 that Rybnik has a higher operating atmospheric pressure and a higher efficiency due to the existing steam reheat circuit. These two parameters cause the volumetric flue gas flow rate of Camden compared to Rybnik to be higher by approximately 20%. It is also shown in the table that the Camden and Rybnik furnace exit gas temperatures are comparable.

Fig. 5a and 5b compare the dimensions of the Camden and Rybnik boilers as well as the temperature distribution within the furnace. The combustion chamber cross-sectional area for Rybnik power plant is 173.8 m² (19.2 m × 9.1 m) while for Camden it is 130.7 m² (13.7 m × 9.5 m). In addition to the comparative atmospheric pressure and efficiency effects, the smaller Camden combustion chamber cross-sectional area causes the flue gas volumetric flow rate to be higher by approximately 33% when compared to Rybnik power plant. The cumulative effects of atmospheric pressure, efficiency difference and combustion chamber cross-sectional area results in a flue gas velocity for the Camden boiler which is almost twice that of the Rybnik boiler. The particle residence time is proportionately reduced for the Camden boiler to be almost half that of the Rybnik boiler as shown in Table 1. The higher combustion chamber flue gas velocity tends to raise the fireball for Camden as shown in Fig. 5a compared to Rybnik Fig. 5b. In addition to the abovementioned effects, the northern hemisphere coals used at Rybnik are far more reactive than those used at Camden and thus have a much lower burnout time.

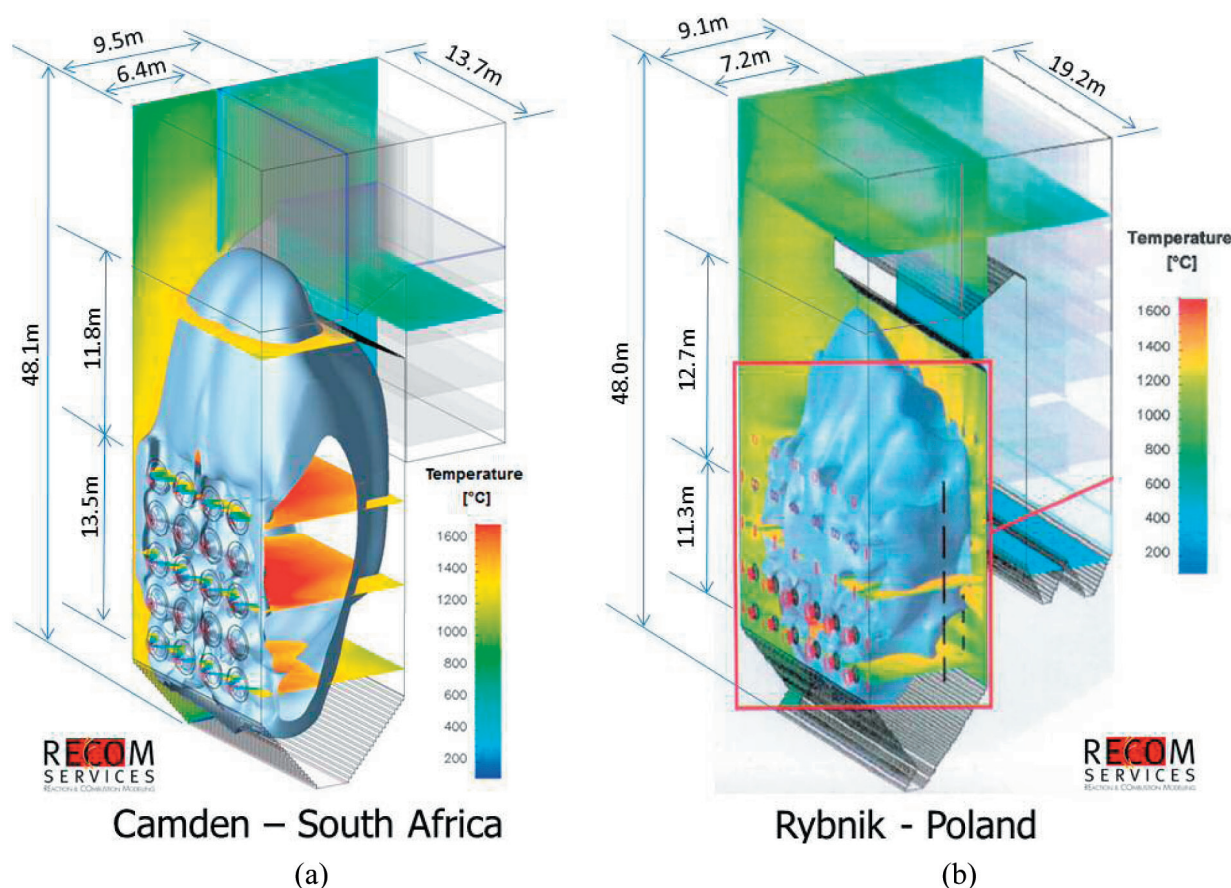


Fig. 5. CFD comparison of furnace temperature distribution on 1400°C iso-surface for Rybnik (acknowledgment to Rybnik for providing the calculation results) and Camden power plant boilers

The CFD calculated mean furnace exit gas temperature for Camden is 1418°C while for Rybnik this value is 1244°C. The 1418°C mean furnace exit gas temperature calculated for Camden is greater than the mean pyrometer measurement (1264°C) and the design value (1166°C) as shown in Table 1.

The CFD calculated value for Camden is also significantly higher than the PFM calculated value of 1254.8°C. The large difference in furnace exit gas temperature between the pyrometer measurement (1264°C), PFM (1254.8°C) and CFD (1418°C) could be generated by assumptions in the CFD model on the char combustion burnout time. The design value is based on OEM empirical correlations while the pyrometer readings and PFM values do not take into account the real temperature profile across the cross-section of the furnace exit.

Considering the furnace residence times and coal burnout time, the Camden boilers seem to be well undersized with regard to the furnace cross section (130.7 m²) and the vertical distance between the burner belt exit and the superheat inlet compared to Rybnik. At Camden, the above issue is further exacerbated by a reduction in volatile matter content from the design value of 24.5%, to the current value of around 20%. This leads to lower flame propagation velocity and delayed particle ignition away from the burner mouth.

4. COMBUSTION SYSTEM

4.1. Secondary air (SA) distribution

Prior to plant de-commissioning in the late 80's, secondary air (SA) supply to the Camden burners was initially achieved through a common non-partitioned wind-box as shown in Fig. 6. Coal is supplied pneumatically via 4 PF pipes at each mill outlet. The primary air (PA) for pneumatic conveyance of the PF is tapped off from the wind-box via a PA to mill Bus Main duct. The SA proportion to each burner is determined by the burner sliding sleeve damper position. With this architectural setup and without automated adjustability of the sliding sleeve dampers on each burner, SA flow control for varying mill loads and combinations could not be achieved. This means that the row of burners out of operation (i.e. mill out of operation) will receive the same amount of SA as burners that are in operation. This results in burners in operation being starved of SA thus impairing their stoichiometry.

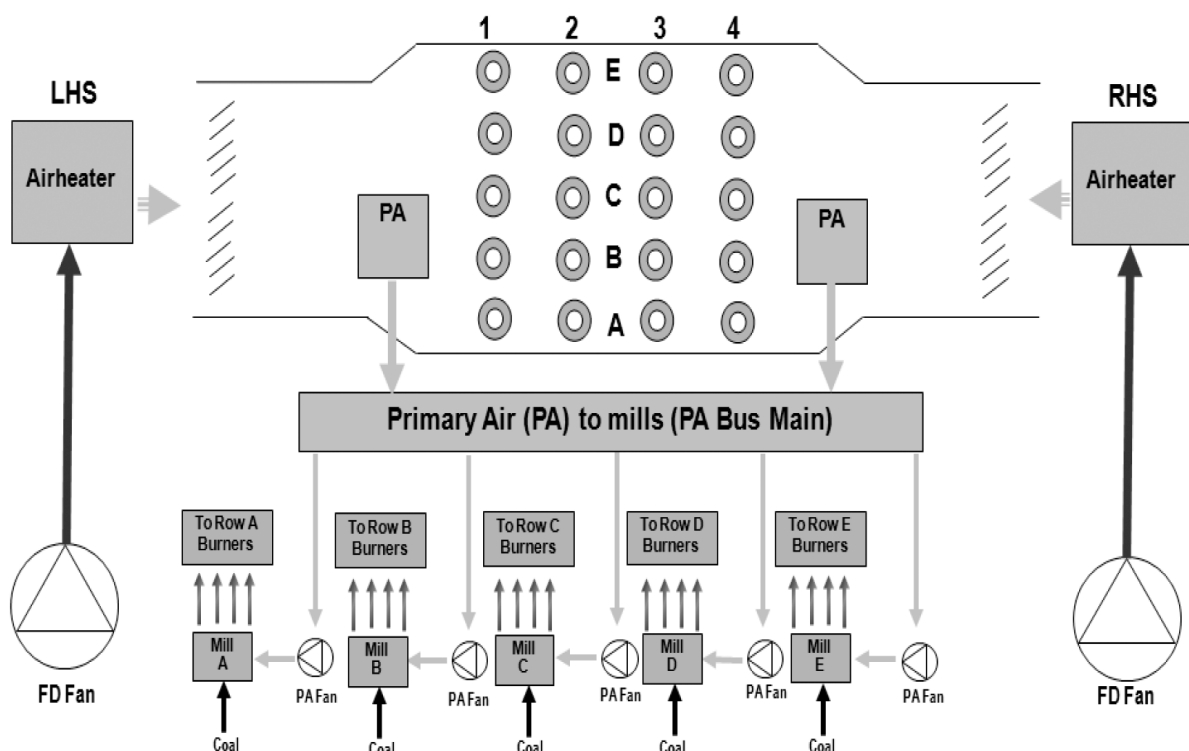


Fig. 6. Wind-box arrangement prior to decommissioning

During return to service and due to problems encountered with SA distribution to the common wind-box, the wind-box was partitioned into five separate levels with wind-box dampers at inlet to each level as is shown in Fig. 7. Furthermore electronic actuation from the control room of the burner SA swirl registers was implemented. To control air flow to each burner level, wind-box/louver dampers which have a controlled opening characterized by the mill feeder speed were also implemented. The wind-box dampers are also controlled to achieve a minimum pressure of 0.4 kPa in the PA Bus Main duct to maintain the necessary PA fan suction pressure.

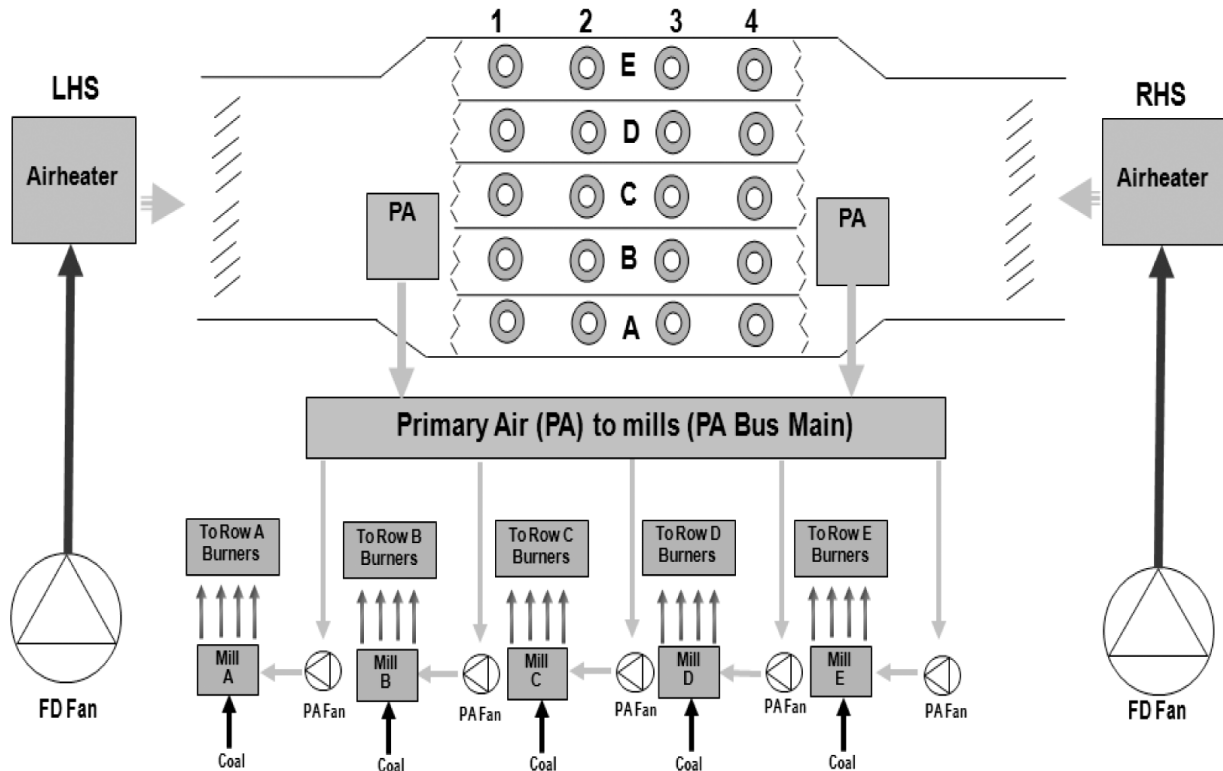


Fig. 7. Wind-box arrangement following RTS modification

4.2. Wind-box air distribution CFD characterization

Through CFD, the pressure drop as a function of the mass flow for varied wind-box damper openings was established. Based on these results, an equation which characterizes the full range of mass flows, pressure drops and wind-box/ louver damper openings was developed. After the wind-box damper characteristics were established, the half-furnace symmetry CFD model also allowed for the evaluation of the efficacy of the damper settings in ensuring even SA distribution to the burner levels within the wind-box system. As shown in Fig. 8, the wind-box dampers and burners are modelled in detail with the latter set to the on-site full load positions as defined in the control system (burner level E out of operation). The burners on the other hand were simulated with a sliding sleeve damper aperture of 70mm and SA swirling register position of 66.67% open. See Fig. 12 for sliding sleeve and SA swirling air register description.

In order to capture any possible effects of temperature stratification within the duct, a velocity and temperature profile to serve as input to the CFD model was generated from traverse measurements at the air pre-heater hot air outlet. Furthermore to simulate the real operating conditions, the total air was proportioned accordingly into PA and SA taking into account the forced draft (FD) fan air flow and air pre-heater leakage measured by onsite flue gas oxygen traverses at inlet and outlet of the air preheater.

Fig. 8 shows both the axial velocity contours on a vertical section through the burner mouth as well as the static pressure contours on a vertical section through the wind-box. It can be seen from the velocity contours that while all the rows have low velocities (dark blue) in the PA/PF pipe due to insufficient core air flow, the idle burner Row E is the worst case with a larger flow recirculation annulus from the furnace back into the PA/PF pipe of the burner.

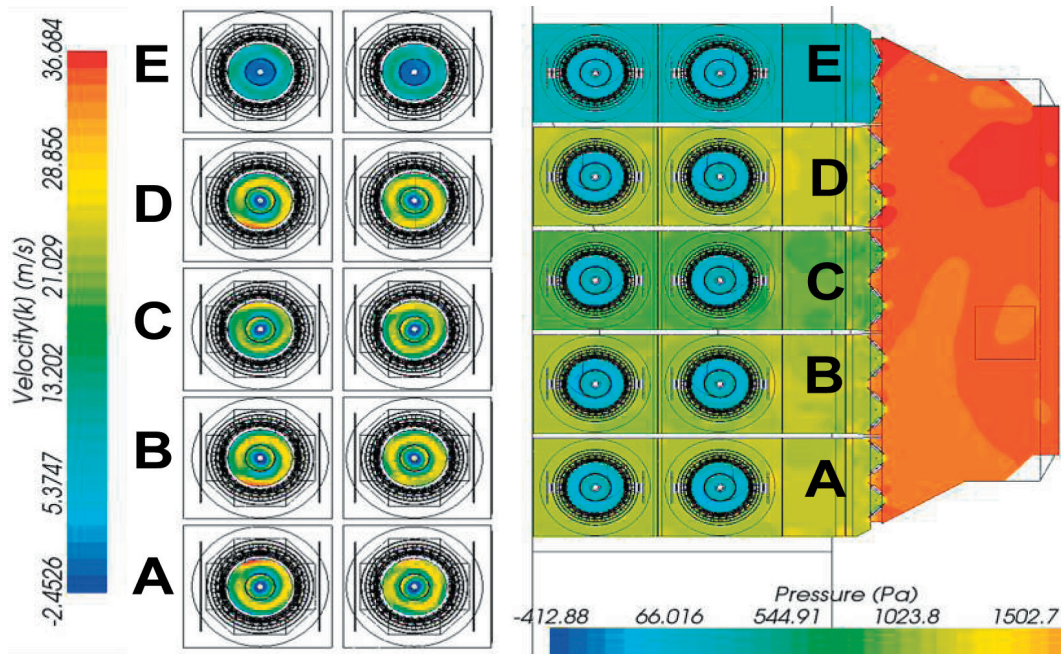


Fig. 8. Half boiler CFD results, Left: Burner axial velocity contours at burner mouth, Right: Static pressure contours

Table 2. Burner mass flows and flow distribution differences

Row	Burner 1 [kg/s]	Burner 2 [kg/s]	Δ 1-2 [kg/s]	Δ 1-2 [%]	Sum 1 & 2 [kg/s]
E	4.3	4.1	0.2	4.7	8.4
D	11.7	11.6	0.1	0.9	23.3
C	10.5	10.8	-0.3	-2.8	21.3
B	11.6	11.6	0	0	23.2
A	11.5	10.7	0.8	7.0	22.2

Table 2 shows the difference in mass flows across the various burner rows. It was observed that on a per row average, Row E which is idle receives approximately 10% of the total SA mass flow to the wind-box. In the CFD calculation (where all burner air control devices are identically set and burner pressure loss co-efficient is identical), relatively well homogenized SA distribution between burner rows is observed.

4.2.1. Wind-box

No design information was available for tuning the burner sliding sleeve dampers, SA swirling registers and wind-box dampers for varying coal quality and boiler load. This design data had to thus be developed before the air control devices could be correctly set. To this end wind-box and burner CFD characterizations were carried out on a two-burner and half-boiler symmetrical wind-box model.

Furthermore due to the unavailability of data, the aim of the CFD modeling was to characterize the wind-box dampers to use them as flow measuring devices to determine distribution of air-flow to each level of the wind-box. The key characteristic parameters that were studied were namely the mass flow of air through a wind-box damper for a given opening and the resulting pressure drop. Fig. 9 shows the CFD characterization of pressure loss across the wind-box dampers as a function of mass flow rate for various wind-box damper positions.

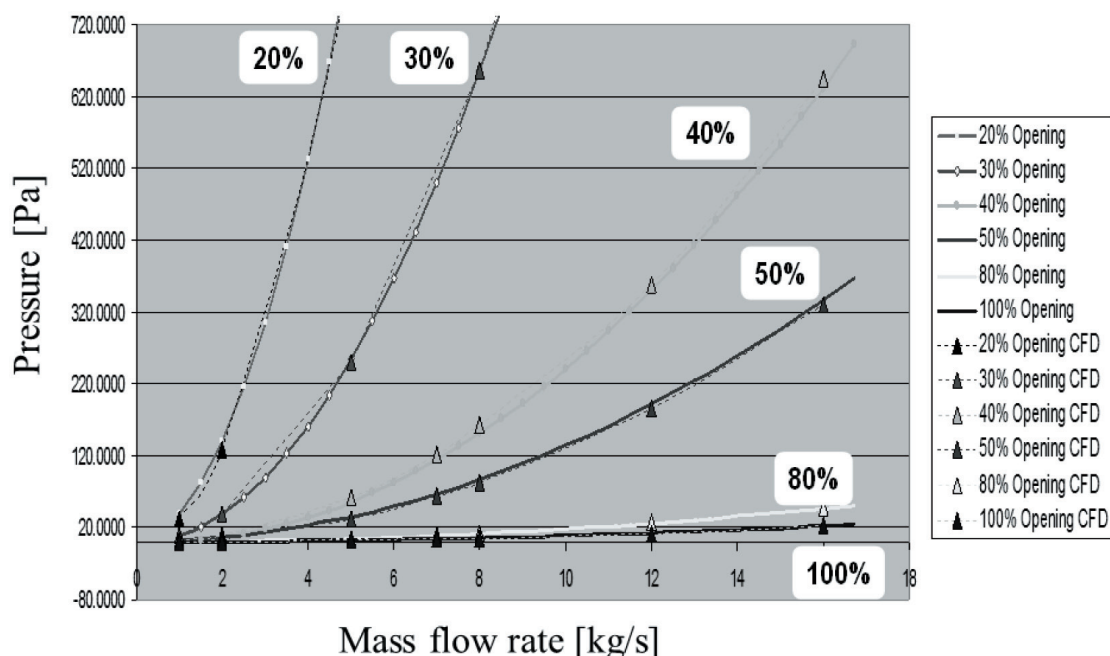


Fig. 9. Comparison of CFD curves vs. the results obtained with a single 3-D equation to characterize the wind-box dampers

4.3. Coal distribution

As repeatedly indicated by post RTS iso-kinetic sampling results, many boilers at the power plant suffered from poor coal distribution between PF pipes exiting a single mill. A decision was made in the framework of the post RTS work to implement on-line PF flow and particle size measurement on the boiler selected as the pilot (unit 2). A coal flow characterization measurement system was installed and commissioned on all PF pipes on boiler 2 during an outage. To obtain PF mass flow in the PF pipes, the mass concentration of PF and velocity of PF are required. The on-line PF flow system measures the velocity of pulverized coal particles by a time-shift of stochastic electrostatic charge signals between two sensors at a known distance apart. For concentration measurement, the pipe acts as a microwave waveguide, which is affected only by PF concentration. The exact frequency of the microwave energy depends upon the pipe's geometry. Deviation of resonant frequency with PF loading forms the basis of the concentration measurement.

The main benefit of the on-line PF flow measurement system compared with the iso-kinetic sampling method is that iso-kinetic sampling is neither an automatic nor on-line measurement system. It is also difficult to envisage having measurements taken simultaneously on all pipes of a single mill with the iso-kinetic PF sampling probe, not to mention to be able to measure all pipes of all mills on one boiler simultaneously. Shown in Fig. 10 is the layout of the 20 on-line PF measurement instruments. The measurement points are installed on vertical, horizontal and inclined pipes, depending on location suitability and access. The PF pipes are numbered 1 to 4 from left to right when looking at the furnace front wall. The mills are labeled A to E depending on the burner level which they feed. Level E is the uppermost level of burners while level A is the lowermost level.

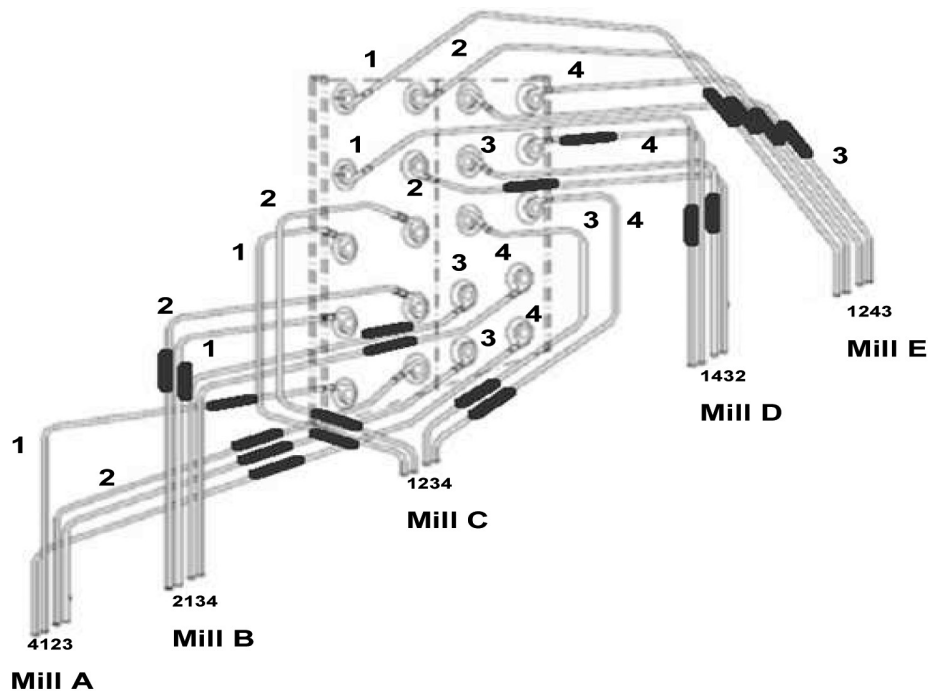


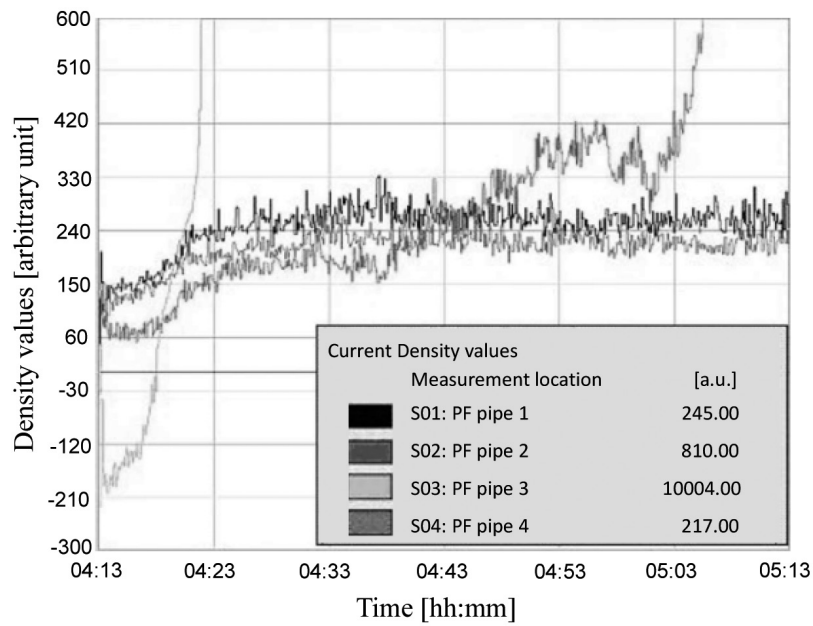
Fig. 10. PF pipe layout and numbering and on-line PF sensor installations (red)

To complement the online PA/PF flow measurements, an on-line Particle Size Analyzer (PSA) has also been acquired from which measurements can also be compared to the results of the PF iso-kinetic probe. After being inserted into the PF pipe, the PSA delivers a continuous particle size distribution within a few seconds delay, while the PF iso-kinetic probe averages the measurements over a few tens of minutes and the sample has to then be taken to the laboratory to be sieved and dried before a result is available. Furthermore, the PSA probe can be kept in a PF pipe for a few days after which it has to be removed to prevent erosion. It is obvious from the measurement procedure that the iso-kinetic probe is not adequate for establishing dynamic characteristics of the mills under varied mill throughput, PA flow, classifier settings etc. With the PSA system this is possible and it is endeavored to become standard control equipment to allow for a condition-based maintenance schedule of the mills rather than a time or failure based maintenance as it is now (Archary et al., 2012).

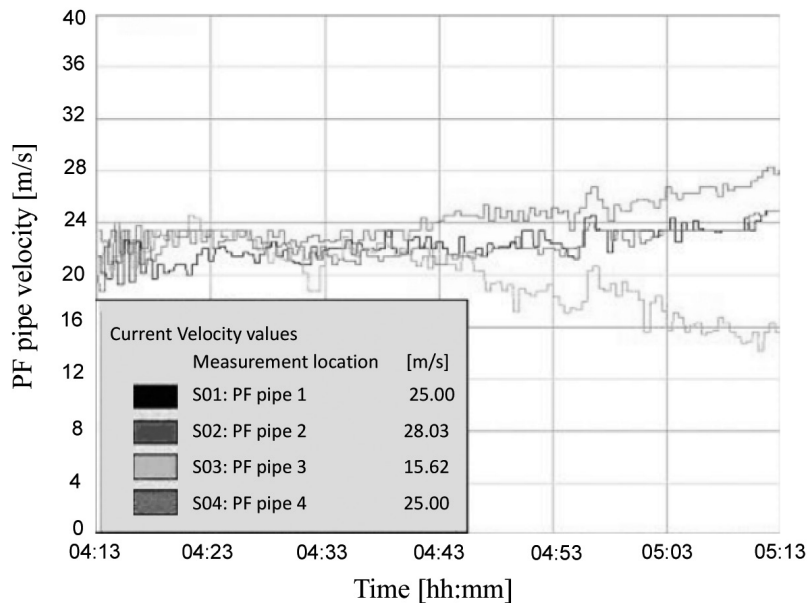
4.3.1. PF flow measurement per PF pipe

To promote improved stoichiometry at the burner, it is necessary to ensure homogeneity of primary air (PA) and pulverized fuel (PF). Inhomogeneous PA and PF distribution will not only affect burner stoichiometry but will also cause reduced pneumatic conveying velocities of PF in affected pipes. Depending on the magnitude of the reduced velocities, this can result in PF settling (saltation) in horizontal pipes (van der Merwe et al., 2012).

Fig. 11a shows a graph of coal concentration vs. time in each PF Pipe of Mill A, as directly given by the on-line PF system. Following purging of the PF pipes with a sudden increase in mass flow rate, it can be seen shortly after the beginning of the time period that the concentration in PF pipe 3 increases abruptly until it is out-of-scale. It is inferred that PF settling occurs in this pipe as the concentration reduces to that similar to the other pipes during purging. It can then be seen in Fig. 11b that over the same time period, the velocity in pipe 3, reduces steadily reaching 16 m/s at the end of the time period. This indicates that it is likely that after purging PF settling steadily increases in this pipe causing the pipe pressure loss coefficient to increase which results in preferential flow to the other pipes which as a consequence see increasing velocities due to the mass flow rate lost in pipe 3. The settling inferred from the measurements in PF pipe 3 was indeed observed by isolating, opening and visually inspecting the pipe. Furthermore, the PF settling contributes to the unsafe operating condition of the burner which is demonstrated in the section hereafter.



(a)



(b)

Fig. 11. Online PF pipe concentrations and velocities

5. BURNERS

5.1. Burner design

The ICAL R-type burners (16 in operation to achieve full load) are supplied with PF by 5 vertical spindle LOPULCO coal mills, with 4 PF pipes at each mill outlet supplying a single row of 4 burners. The main measures existing for controlling burner combustion in the original plant were:

- Total air flow at forced draft (FD) fan outlet – annubar measurement
- Total coal flow at feeder – volumetric measurement
- Total PA flow to a mill – calculated from fan motor current
- Wind-box static pressure measurement
- Burner sliding sleeve damper opening

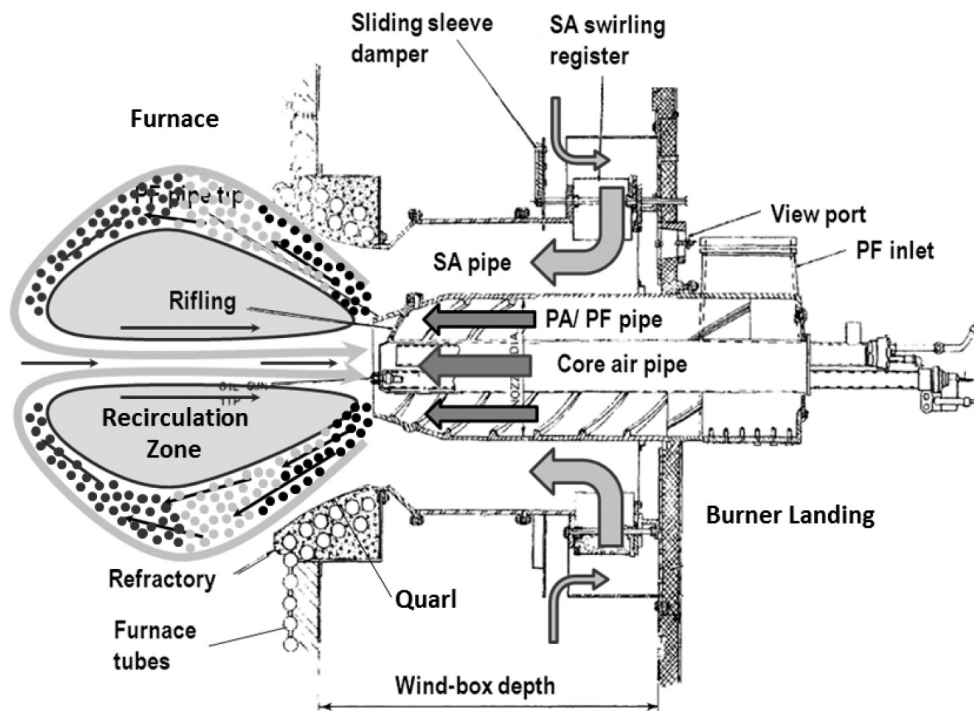


Fig. 12. R-type burner nomenclature and general arrangement

Fig. 12 shows the burner components with functions as follows:

- *Sliding sleeve damper*: Aimed at controlling SA distribution between burners
- *SA swirling registers*: Aimed at swirling the SA to create a flue gas recirculation zone in the furnace in front of the PF pipe tip to accelerate heat flux to the incoming PF in order to enable rapid devolatilization of the PF within the burner quarl
- *SA pipe*: Conveys SA from wind-box to furnace
- *PA/PF pipe*: Pneumatically conveys PF from mill outlet to furnace
- *Core air pipe*: Conveys core air for burner oil firing during start-up or PF ignition support.

The burners have had a history of drawbacks associated with overheating, PF settling and poor secondary air (SA) distribution to the wind-box levels, dating back to pre-decommissioning days. These lead to cracking of the cast-iron PF pipe tips and SA pipe, combustion within the PF pipe tip and rear region of the SA pipe (Peta et al., 2012).

5.2. Burner flow and temperature measurement installations

To investigate the drawbacks prevailing within the burners, measurement and CFD analysis have been employed. With respect to measurements, bi-directional total pressure impulse line with associated gauges have been installed in each SA pipe of burner levels A, C and E of the wind-box as shown in Fig. 13. Furthermore thermocouples have been installed within all the burner PF and SA pipes on the outer and inner surfaces respectively and on all burner levels. The bi-directional total pressure tubes are installed in the direction of the burner center-line at 2 O'clock and 10 O'clock radial positions as seen when facing the boiler front wall. This installation resembles that which has been performed at Allegheny Energy Supply's Armstrong power plant in the USA (Brown, 2004). The total pressure tubes are connected to a differential pressure gauge which gives a positive differential pressure for flow from the burner into the furnace and a negative differential pressure for flow from the furnace into the burner. Furthermore, the aim of the bi-directional total pressure tubes is to obtain an indicative measurement of flow distribution between burners on a single burner level. The thermocouples are used as an additional sensor to monitor burner metal temperatures over varying boiler loads, air flows and mill combinations.

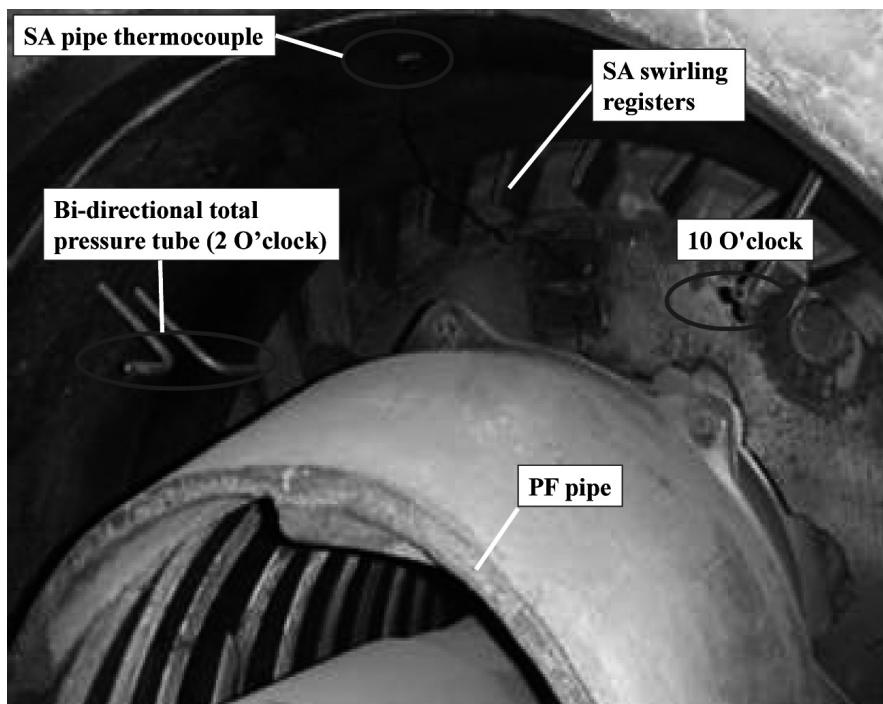


Fig. 13. Burner SA pipe bi-directional total pressure tube installation

5.3. Burner flow and temperature measurement results

Burner CFD calculations to characterize the burner mouth flow dynamics were performed. The main aim of the calculations was to determine whether flow recirculates from the furnace into the burner. It was shown by CFD that indeed flow recirculation from the furnace into the burner occurs. Furthermore it was shown that depending on the burner SA swirl setting it can either occur on the outer periphery of the SA pipe or otherwise the inner periphery. A summary of the results shows that flow recirculation into the burner can be expected in all regimes of burner operation. This leads to damage of the cast iron PF pipe tip and SA pipes due to overheating by flue gas. Also evident is that the global flow recirculation into the burner occurs at localised regions of the burner mouth outlet. This explains why the bi-directional total pressure tubes installed on rows E,C and A did not indicate flue gas recirculation on all occasions that it occurred although thermocouples installed on the burners indicated sudden extreme temperature excursion. This hot flue gas recirculation into the burner will bring with it burning/un-burnt fuel into the burner posing a burner/ wind-box fire risk. Shown on the Fig. 14 and Fig. 15 is a study of a burner overheating incident in which gas flow recirculation into the burner.

Fig. 14 shows the differential pressures given by each of the pairs of bi-directional total pressure tubes installed in the SA pipe of burner E1. It can be observed on the time axis at about 12h20 that the pressure gauge indicates flow recirculation into the burner. Shortly afterwards as shown in Fig. 15 the SA and PF pipe thermocouple measurements show a step increase in temperatures. The temperature in the SA pipe reaches a peak value of approximately 1000°C at about 16h00 on the timescale. At about 16h30, overheating of the wind-box was visually observed externally during a routine inspection and fuel isolation immediately initiated (Peta et al., 2012).

6. ON-GOING WORK

To master the air flow control to single burners and between burner levels, a CFD approach is under development in which the burner itself is used as an air flow measurement device. This approach involves

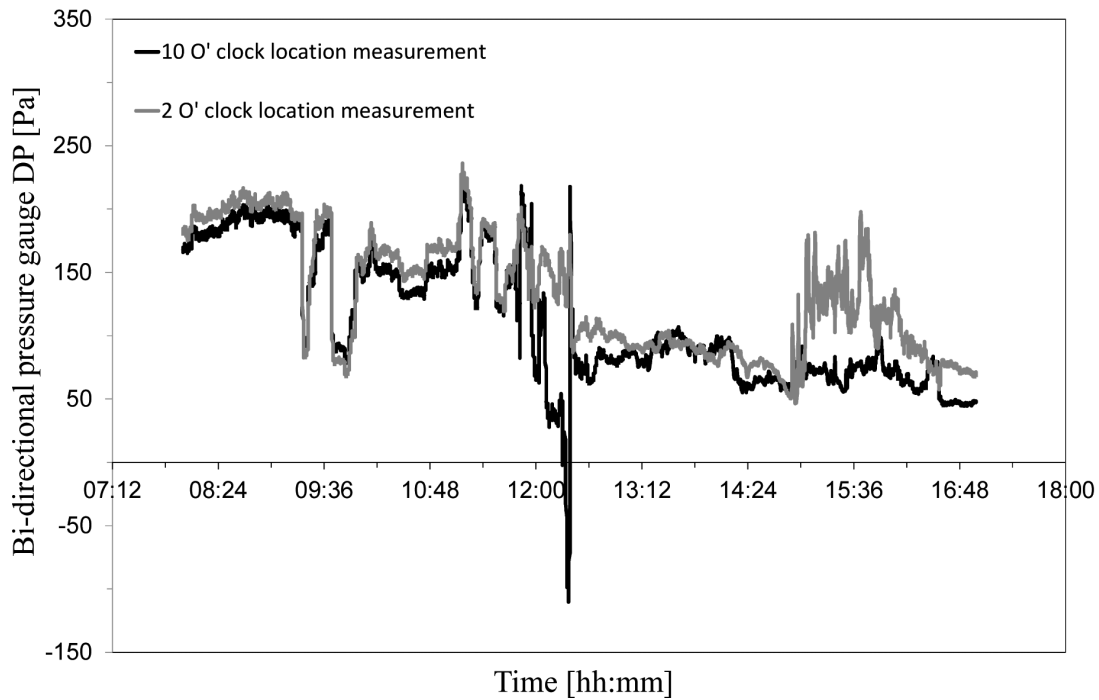


Fig. 14. SA pipe differential total pressure measurements

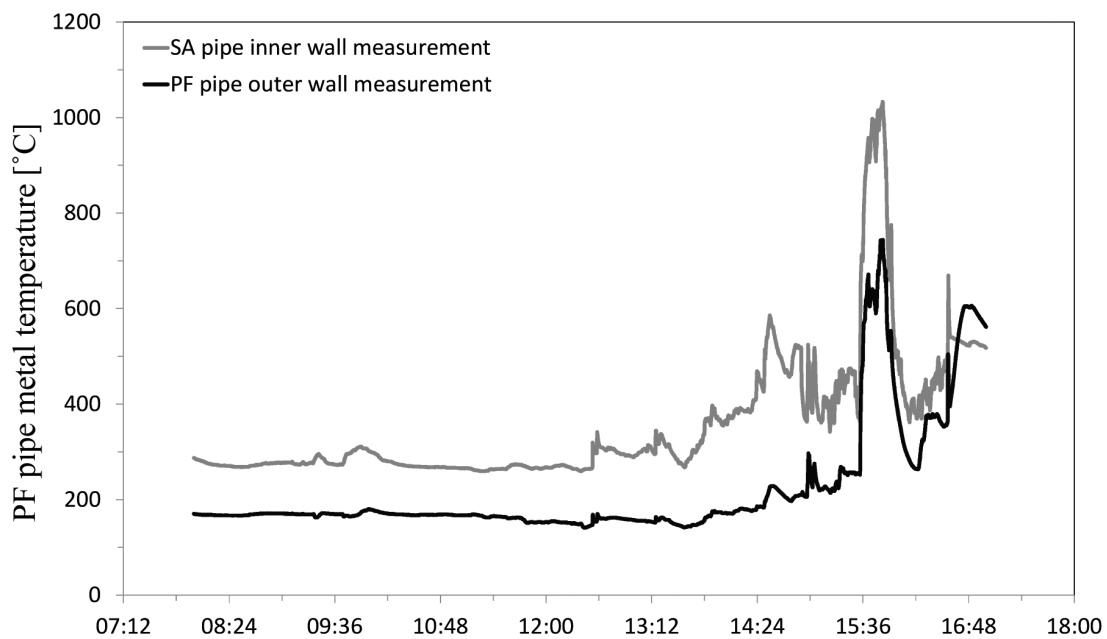


Fig. 15. SA and PF pipe thermocouple measurements

characterizing the air flow through the burner annuli for varied load conditions and burner air control device settings. Static pressure measurements on the burner are used to validate the model characterization. It is envisaged that the validated characterization be incorporated into the control system for single burner air flow measurement and control.

7. CONCLUSIONS

The results of the boiler design review, PFM and CFD calculation, indicate that the Camden boilers are undersized with regard to furnace cross-section and the vertical distance from the burner belt exit to the superheater inlet which determines the furnace residence time. The coal particle burnout time is shown to

be greater than the furnace residence time. This results in higher than design furnace exit gas temperature which causes metal temperature excursions at the superheater inlet and FFP inlet.

Furthermore an integrated methodology starting at the global boiler level to determine the portion of total air fractioned towards air pre-heater leakage, tramp/ ingress air, PA and SA between burner levels and between burners on a single row has been developed. The use of single burner measurements for fault diagnosis has also been demonstrated as well as their potential for use as air flow measurement devices by CFD characterization has been identified.

The gross inhomogeneous distributions of total air, PF, PA and SA that can occur within a wind-box system due to air pre-heater leakage, tramp air, fuel distribution, mechanical air control device settings and the need for single burner air flow measurement has been demonstrated. From the characterizations performed, air control device settings for SA distribution between burners on a single level have been proposed. The installation of a differential static pressure measurement between the upstream and downstream wind-box dampers gives additional measurements for improved control of air to burner levels.

Following the post RTS investigative work and operational experience of burner drawbacks that continue to exist, it has been decided to retrofit the burners. This nowadays necessitates the installation of Low NOx burners which comply with current South African environmental legislation with regard to NOx emission limits. This extensive work on an aged boiler serves as feedback experience for the road to be travelled in order to have mastery of global coal and air flow to the combustion system as well as to single burners. The air and coal mastery being especially crucial when embarking on Low NOx burner retrofit strategies.

The authors would like to thank the engineering and performance and testing staff of Camden Power Plant for their operational experiences and invaluable contributions to these studies. For the data on Rybnik Power Plant which enabled benchmarking of Camden Power Plant, the authors would like to express their gratitude to Krzysztof Szczepanek. RECOM Services and Steinmüller Engineering GMBH are also acknowledged for the combustion CFD calculation and Process Flow Modelling results respectively.

REFERENCES

- Archary H., Jestin L.M., Roohani H., 2012. Online measurement and condition based maintenance of pulverised fuel vertical spindle mills. *POWER-GEN AFRICA 2012*. Johannesburg, South Africa, 6-8 November 2012.
- Brown R., 2004. *Coal and air flow measurement and control at Allegheny's Armstrong Station*. EPRI, March 29, 2004. Available at: <http://www.epri.com/abstracts/Pages/ProductAbstract.aspx?ProductId=00000000001009374>
- Department of Trade and Industry, 2001. *Technology status report. Pulverised fuel (PF) flow measurement and control methods for utility boilers*. Available at: <http://webarchive.nationalarchives.gov.uk/+http://www.berr.gov.uk/files/file19294.pdf>.
- Peta S., du Toit C., Jestin L.M., Roohani H., 2012. Burner flow controls for safe, reliable, complete and clean combustion. *POWER-GEN AFRICA 2012*. Johannesburg, South Africa, 6-8 November 2012.
- van der Merwe J.C., Roohani H., Jestin L.M., Simonin O., van Wyk C., Archary H., 2012. Mastering pulverised fuel distribution to low-NOx burners for safety and environmental protection. *POWER-GEN AFRICA 2012*. Johannesburg, South Africa, 6-8 November 2012.
- Winkler H., 2006. *Energy policies for sustainable development in South Africa. Options for the future*. Energy Research Centre, University of Cape Town. Available at: https://www.iaea.org/OurWork/ST/NE/Pess/assets/South_Africa_Report_May06.pdf.

Received 11 March 2015

Received in revised form 21 July 2015

Accepted 23 July 2015